

JSACE 1/28

Study of Four Passive Second Skin Façade Configurations as a Natural Ventilation System During Winter and Summer

Received
2020/09/24

Accepted after
revision
2021/03/15

Study of Four Passive Second Skin Façade Configurations as a Natural Ventilation System During Winter and Summer

Youssef Hamidi*, Mustapha Malha, Abdellah Bah

Mohammed V University in Rabat, École Nationale Supérieure D'arts Et Métiers, ENSAM, B.P.6207, Rabat, Morocco

*Corresponding author: youssef.hamidi@um5s.net.ma

 <http://dx.doi.org/10.5755/j01.sace.28.1.27728>

The fight against climate change is a significant challenge, resulting mainly from the linear and extensive exploitation of natural resources, particularly fossil fuels. Its impacts are now recognized. The current climate models are neither sustainable nor ecological in economic and social terms, especially as we live in a century marked by galloping demography and urbanization. Researchers worldwide have paid great attention to passive solar design strategies such as double skin or Second Skin Façade.

From this point, the present work aims to contribute to a better understanding of the feasibility of using a passive façade as a useful technology for natural ventilation to achieve potential energy savings and improve thermal comfort and indoor air quality. For this purpose, a parametric study was conducted for a room with four different southern facade configurations in six Moroccan climatic zones; the difference between each lies in the vent's position in the entrance and exit. This process was done by using COMSOL Multiphysics software. Velocity and volume flow rate fields were analyzed. The proposed configurations provided an average volume flow rate between 200 m³/h and 400 m³/h for a surface of 1 m² of southern façade with an air vent area of 0.1mx0.2m.

Keywords: Solar Passive Design; Building Energy Efficiency; Trombe Wall Passive Second Skin Façade; Natural Ventilation; CFD Simulation.

List of symbols

ρ :	Density [kg/m ³]
C_p :	Specific heat capacity at constant pressure [J/kg. K]
T :	Temperature [K]
q :	Heat flux (W/m ²)
u :	Velocity (m/s)
P :	Pressure (Pa)
Q :	Heat sources
$\mathbf{1}$:	Thermal conductivity (W/(mike))
$P_{rT\infty}$:	Prandtl number at infinity
T :	Temperature [K]
I :	Identity tensor
In:	Indoor
Out:	Outdoor



Global warming could reach 1.5 degrees Celsius between 2030 and 2052 (Masson-Delmotte et al., 2018); owing to its severity and global threat, it has become a strategic issue worldwide, likely due mainly to massive population growth and industrialization.

The greenhouse's significant responsibility for the widespread gas emissions lies with residential and non-residential buildings. Here we focus on Morocco's case where buildings account for 36% of the final energy consumption (AMEE, 2019). Heating, ventilation, and air conditioning (HVAC) systems take the most power consumption to fulfill indoor thermal comfort. As increasingly demanding conditions impose, the energy efficiency measures are now one of the significant challenges architects and researchers face. In addition to providing power significantly, it also allows for adequate internal comfort conditions.

The focus of green building development is using renewable energy for building energy conservation. Researchers favor the most important renewable energy, passive solar strategies, because of its abundant reserves, convenient development, and utilization. One of these strategies that recently received significant attention because of its multiple applications is its specific construction package known as the double-skin façade, Second Skin Façade, or Passive Façade like Trombe walls and solar chimneys (Du et al., 2020a; Poirazis, 2004).

Trombe wall can be used either for passive cooling, heating, or natural ventilation. In 1881, E.S. Morse first patented this wall, then both Felix Trombe and Jacques Michel developed and popularized it (Trombe & Michel, 1972). It consists mainly of double skin separated by a ventilated cavity, an external glass, and a thermal mass, which is often painted black on the outside. The absorption of solar radiation is enhanced, resulting in airflow through the building by buoyancy effects.

The main Passive Façade structural elements include glazing, cavity, a massive wall, coating color, heat insulation, air ducts, and windows in a massive wall. According to (Prieto et al., 2018; Vučenović et al., 2013), when designing a Passive Façade project for specified climatic conditions, the designer must consider each element's technical and economic parameters. Many investigations on the main structural elements of a Passive Façade and their influence on investigators' efficiency were conducted. Glazing has a significant impact on the accumulating efficiency of the passive façade. This point is since a double-glazed skin can reflect and absorb some part of the spectrum of solar radiation; consequently, the most efficient is the use of double-glazing skin with low-emittance in the façade (Prieto et al., 2018; Zalewski et al., 2002). Among the other most critical aspects studied in the literature are the following: Air gap (Chen et al., 2006; Du et al., 2020b; Parhizkar et al., 2020), Massive wall and Heat insulation (Hu et al., 2020; Liu et al., 2020; Nizovtsev et al., 2020).

Trombe's tremendous success has been reducing energy demand in cooling and heating in residential and commercial buildings. According to numerous studies of its impact (Lin et al., 2019; Long et al., 2019; Yu et al., 2019; Zhou et al., 2019). Regarding passive heating, in work presented by (Chel et al., 2008), a building energy simulation (BES) using TRNSYS software of a honey storage building with a Trombe wall located in Gwalior (India) was carried out. During the winter months, the building's ambient air temperature falls below the required temperature range of 18 °C and 27 °C, suitable for honey storage. The Passive Façade has proven to be a Natural Heating system with energy conservation up to 3312 kWh/year with a 15 m² wall area.

Similarly, (Jaber & Ajib, 2011) investigated the effect of the Trombe wall area ratio relative to the south wall's total area on the building's heating from a thermal and economic point of view using the life cycle cost (LCC) criterion. They found that the portion of heating energy savings increased with increasing the Trombe area ratio; for a 20% ratio, approximately 22.3 % of the auxiliary heating energy was saved annually. However, when this surface exceeded 37 %, heating energy savings remained at almost constant values, 32.1% of energy savings. These findings are in good agreement

with the numerical and experimental study conducted by (Abbassi et al., 2014) in which a significant reduction of the total heating demand by a value of 77 % approximately was achieved with an 8 m² Passive Façade for a 16 m² simple typical building in Tunisia.

Whereas Passive Façade has proven to be beneficial concerning heating, some researchers such as (Bajc et al., 2015) have shown that the Passive Façade can be an additional source of thermal loads in summer conditions; they carried out a 3D Computational fluid dynamics (CFD) under ANSYS software of a room with a southern passive façade, protected by photovoltaic stripes, during a typical summer day. Thus, to enhance passive cooling, several authors (Hong et al., 2019; Stazi et al., 2012) emphasized the importance of solar shading (overhangs, roller shutters, and Venetian blinds) of the Façade in summer.

However, the Passive Façade's effectiveness in enhancing natural ventilation did not appear to receive the same amount of attention, as did the study analyze the heating/cooling potential of Passive Façades. Nevertheless, the airflow was rarely analyzed. The air velocity variation has an essential influence on the natural ventilation, heating, and cooling potential of Passive Façades.

Given this literature gap, this study aims to obtain the velocity distribution and the airflow rate in a Passive Second Skin Façades. A comparative study of four different Passive Façades configurations across a range of Moroccan climatic zones to identify the optimum configuration inducing better indoor natural ventilation and improving thermal comfort was carried out to achieve the study's objective. The mathematical description and CFD simulation results are given in this article, and the results are analyzed and discussed in depth.

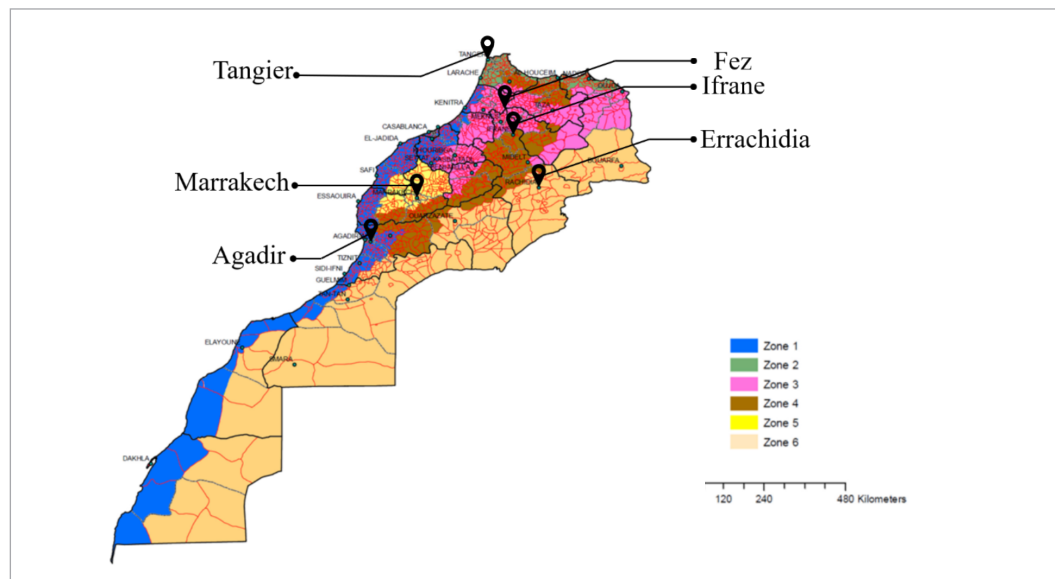
Materials and Methods

Meteorological data

Meteorological data for six Moroccan climates were studied with a view order to obtain a wide range of climatic conditions. The study was conducted in the following areas: Zone I (Agadir), Zone II (Tangier), Zone III (Fez), Zone IV (Ifrane), Zone V (Marrakech), and Er-rachidia (Zone VI) (see Fig. 1) for which weather files (ASHRAE 2017) are available directly via the 'Heat Transfer interface' on COMSOL Multiphysics software (AB, 2020). The hourly air temperatures and solar radiation represented meteorological data of particular interest. Typical winter periods (January 2nd) and summer (August 2nd) have been selected for simulations in winter and summer conditions. Fig. 2 and 3 show the global solar radiation and ambient temperature in each studied climatic zone during summer (a) and winter (b).

Fig. 1

Six Moroccan climates



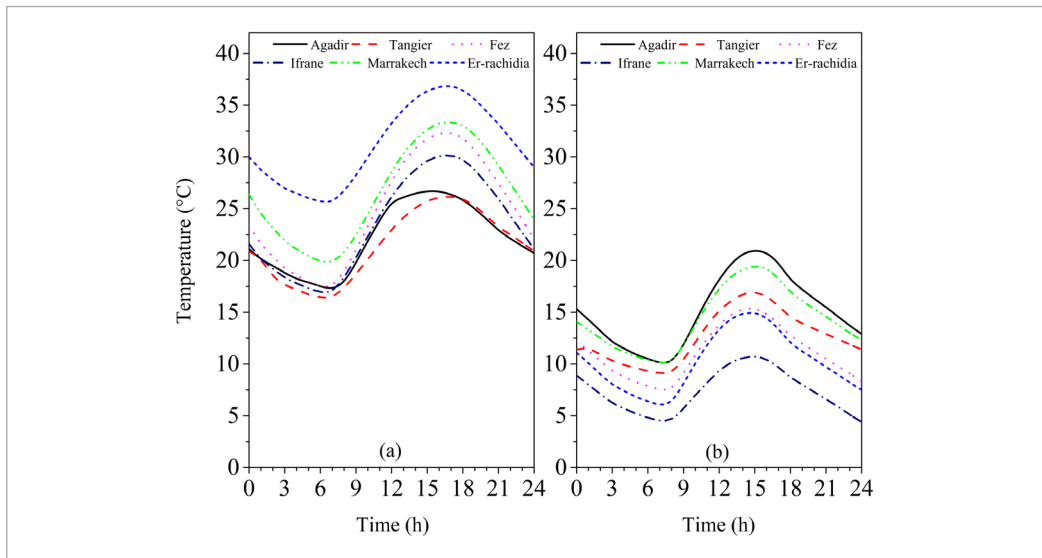


Fig. 2

Typical day's ambient temperature in the six cities: August 2nd(a) and January 2nd (b)

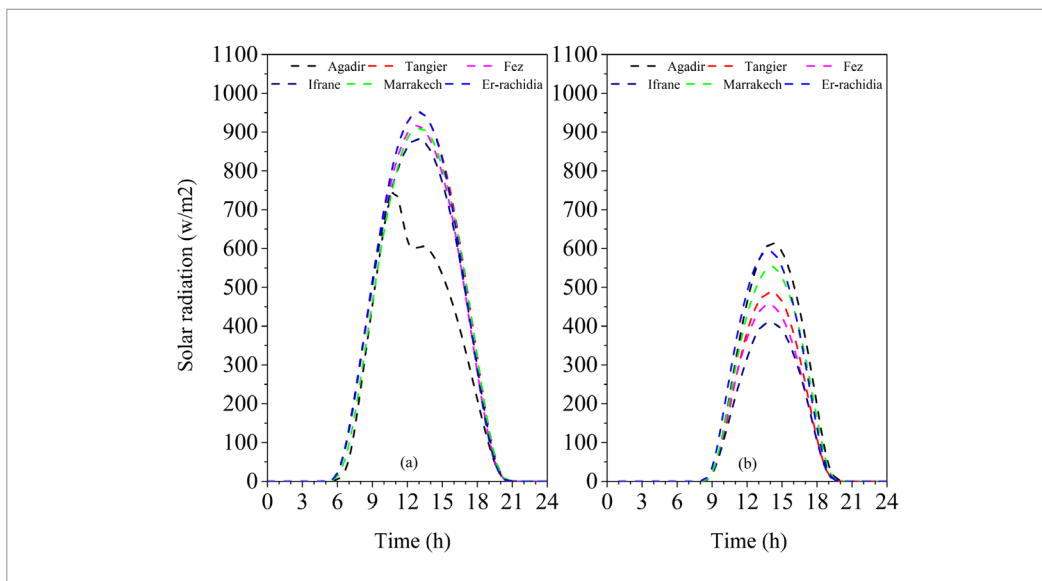


Fig. 3

Typical day's solar radiation in the six cities: August 2nd(a) and January 2nd (b)

Cell description

For optimum control of the study, a virtual model of a test cell 1.261 m in length, 1.112 m wide, and 1.112 m high with southern passive Second Skin Façade was developed. It consists of the outer to the inner side of the 0.005 m glass, a 0.1 m air gap, and a concrete wall 0.1 m thick with 5 cm thermal insulation of expanded polystyrene, as shown in Fig. 4-a. Like the constructions of other walls, we can quickly notice that the floor and roof are made of 0.018 m thick plywood with expanded polystyrene insulation (0.02 m thick) between sheets.

We have set up four different configurations of the passive façade by putting the analyses and numerical comparisons based on four different air vent positions. They have been defined as:

- Case 1 - Out-In configuration: in this case, we find that one air vent is at the bottom of the glazed skin similar to the other, which is sated at the top of the massive wall (Fig. 5-a);
- Case 2 - In-Out configuration: in this case, we find that the massive wall is with a lower air vent and in the glazed skin an upper air vent on the (Fig. 5-b);

Fig. 4

The studied cell's description:
(a) 3D-view,
(b) floor-plan

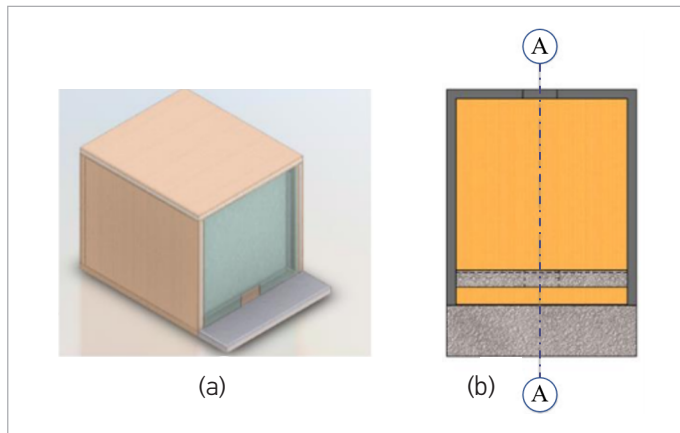
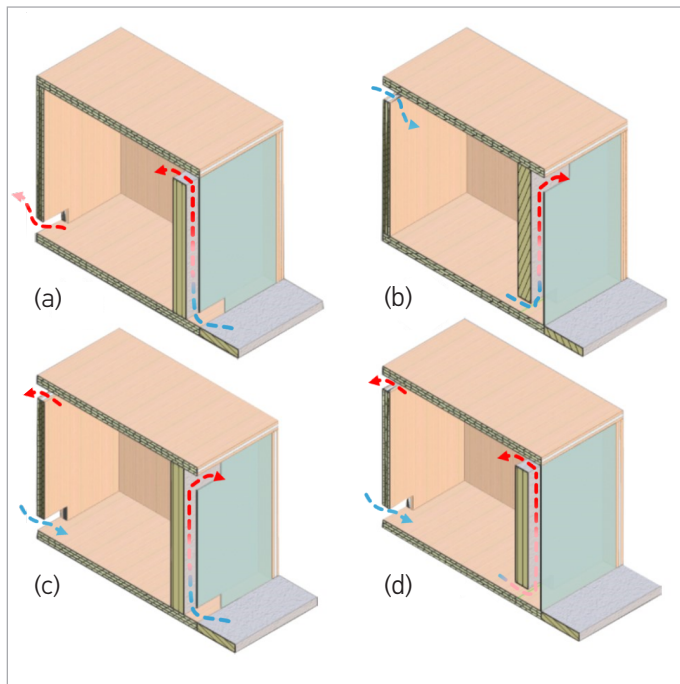


Fig. 5

Cross-section of the studied configurations:
Case 1 (a), Case 2 (b), Case 3 (c),
and Case 4 (d)



- Case 3 - Out-Out configuration: the glazing skin, in this case, we find that consists of both air vents (Fig. 5-c);
- Case 4 - In-In configuration: in this case, we find that the massive wall's lower and the upper parts of the two air vents are located (Fig. 5-d).

Fig. 5 below presents a cross sectional view of the configuration design detailed as follows A-A (Fig. 4-b).

CFD model

In this study, COMSOL Multiphysics software was used. A dynamic three-dimensional model in which Heat Transfer in Solids and Fluids, Laminar Flow, and Surface-to-Surface Radiation physics were coupled through the Nonisothermal Flow and Heat Transfer with Surface-to-Surface Radiation Multiphysics feature. For higher accuracy of mesh generation, an enhancement feature has been introduced. It analyzes the solution's errors and improves the mesh by the results, e.g., for Case 2 configuration, the mesh consists of 357357 domain

41901 boundary elements and 2059 edge elements. The iteration convergence criterion value was set at a 10^{-5} value with a time step of 0.1 h. In this study, time dependent analysis has been performed using the PARDISO sparse direct linear solver. A fully-coupled approach was adopted in which a global Newton-Raphson method was employed.

For the numerical model validation, an experimental study has been carried out with a test cell of 1.261 m x 1.112 m x 1.112 m with a southern passive second-skin façade (see Fig. 6). The same geometrical configuration and thermophysical properties were used. The test cell instrumentation and monitoring, submitted to real weather conditions, qualified to obtain a continuous acquisition of different parameters that characterize the passive façade. Temperature sensors were positioned in the test cell in different locations to measure the air vents' temperature fluctuation, skin surface temperature, and the temperature inside the cell. A thermo-anemometer was used to measure air velocity near the exhaust air outlet. Also, Outdoor conditions were monitored, such as temperature and solar radiation intensity.



Fig. 6

Real image of the experimental test cell

Governing equations

The Fluid Flow module is founded on the Navier-Stokes equations governing the conservation of mass, momentum, and energy, which can be written as follows (Comsol, 2015; Mehrzad Tabatabaian, 2014):

$$\frac{\partial \rho}{\partial t} + \nabla \cdot (\rho u) = 0, \quad (1)$$

$$\rho \frac{\partial u}{\partial t} + \rho(u \cdot \nabla)u = \nabla \cdot [-pI + \mu(\nabla u + (\nabla u)^T) - \frac{2}{3}\mu(\nabla \cdot u)I] + (\rho - \rho_{ref})g, \quad (2)$$

The following equation was given in order to present the governing equation for heat transfer:

$$\rho C_p \frac{\partial T}{\partial t} + \rho C_p u \cdot \nabla T + \nabla \cdot q = Q, \quad (3)$$

$$q = -k \nabla T, \quad (4)$$

To represent the model of convection disorders, kays Crawford has been selected, where PrandTel as assigned:

$$\text{Pr}_T = \left(\frac{1}{2 \text{Pr}_{T\infty}} + \frac{0.3}{\sqrt{\text{Pr}_{T\infty}}} \frac{C_p \mu_T}{k} - (0.3 \frac{C_p \mu_T}{k})^2 (1 - e^{-k/(0.3 C_p \mu_T \sqrt{\text{Pr}_{T\infty}})}) \right)^{-1} \quad (5)$$

Boundary conditions

To evaluate the velocity and the volume flow rate, we have considered the following hypotheses:

Regarding fluid flow, the following assumptions have been considered:

- _ We considered a laminar and weakly compressible flow;
- _ All rigid surfaces were not treated with slip conditions;

In regards to the heat transfer and Surface-to-Surface Radiation modules in which:

- _ Black painted surface (absorber) was treated with diffuse surface boundary condition, with an emissivity of 0.95;
- _ Air vents were characterized as inflow/outflow boundaries;
- _ Heat flux boundary condition was imposed at external surfaces with a heat transfer coefficient of $25\text{W/m}^2 \cdot \text{K}$ that was determined according to (ISO 6946, 1996);
- _ Thermophysical properties of materials are constant;
- _ No moisture inside the room, and hence no evaporative heat source;
- _ The external surface of the room receives solar radiation, which depends on the wall orientation and time.

Results and Discussion

Via a series of simulation calculations, the numerical value of the air outlet velocity and the volume flow rate exchanged between the cell and the outside are obtained. In this section, we will examine the velocity and volume flow rate of the considered configurations in a typical day during winter and summer. Simulation results revealed that the Case 3 configuration was not relevant for natural ventilation. However, in this case, the exchange is made only between the façade cavity and the outside. So, there is no air supply.

Velocity distribution analysis

This section focuses on the upper air vent's continuous process by checking airspeed distribution for case 1 and 4 configurations and in the lower opening for case 2 configuration during the winter and summer typical day. The simulations performed for velocities of configurations of case 1, 2 and 3 suggest two extreme velocities distribution corresponding to two climatic zones:

Zone 1: represented by Ifrane, the coldest city in winter

Zone 2: represented by Marrakech, the warmest city in summer

Air velocities distributions of all configurations in other cities for the same typical day fall between those of Zones 1 and 2.

By reading the details in Fig. 7-b (Ifrane city), the three studied configurations showed significant airspeeds, During the winter with the same evolution, but with different amplitudes; varying between a minimum of 0.28 m/s, 0.33 m/s, and 0.34, respectively, for Case 1, Case 2 and Case 4 confirmations between 05:00 AM and 06:00 AM, and a maximum of 0.31 m/s for the Case 1 configuration, 0.36 m/s for Case 2 and 0.375 m/s for the Case 4 configuration between 01:00 PM and 04:30 PM. As regards the summer season, Fig. 7-a presents that significant airspeeds were generally recorded in the Marrakech city, which attained 0.42 m/s, 0.48 m/s, and 0.51 m/s, respectively, for the Case 1, Case 4, and Case 2 configurations.

We can notice that daytime velocity follows the solar radiation for both summer and winter seasons; the stack effect can explain this due to solar radiation. In contrast, nighttime velocity was low compared to the daytime velocity but generally remains essential because of the massive wall's thermal inertia.

Comparing the amplitude of the airspeed for both seasons, we can see that the amplitude during the summer season is significant compared to the winter season; this is clearly explained by the power of the sun received by the wall, which is about 900W/m^2 in Marrakech during the summer (see Fig. 3-a), while it does not exceed 400W/m^2 in Ifrane during the winter (see Fig. 3-b).

Fig. 8 and 9 show the Velocity field (Streamlines) and velocity magnitude (Surface) of a vertical cut plan at the center of the room at 04:00 PM, respectively, during winter in Ifrane and summer Marrakech. As apparent from Case 4 configuration (Fig. 8), the flow entered through the lower opening of the north façade and exited through the upper opening of the same façade crossing the Passive Second Skin Façade cavity. As for the Marrakech case (Fig. 9), the flow through the opening has been compromised

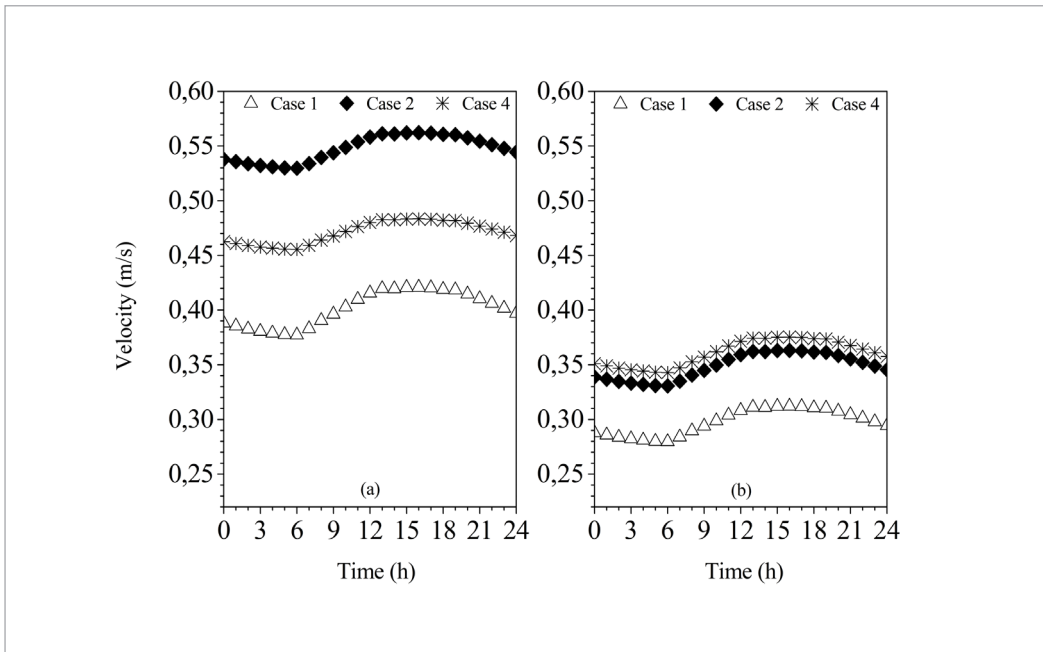


Fig. 7

Outlet velocity distribution during the summer day in Marrakech (a) and the winter day in Ifrane(b)

North facade to exit the glass's top air opening due to buoyancy-effect.

Volume flow rate analysis

After analyzing the velocity distribution in this section, we will first examine the volume flow rate for cases 1,2, and 4 configurations during typical winter and summer days in Ifrane and Marrakech cities. Then we will analyze the volume flow rate for the same configurations in climatic zones 1,2,3,4,5, and 6 represented by respectively, Agadir, Tangier, Fez, Ifrane, Marrakech, and Er-rachidia. All volume flow rate measurements are carried out of the upper air vents for cases 1 and 4 configurations and in the lower air vent of the case 2 configuration with the same area of 0.1mX0.2m.

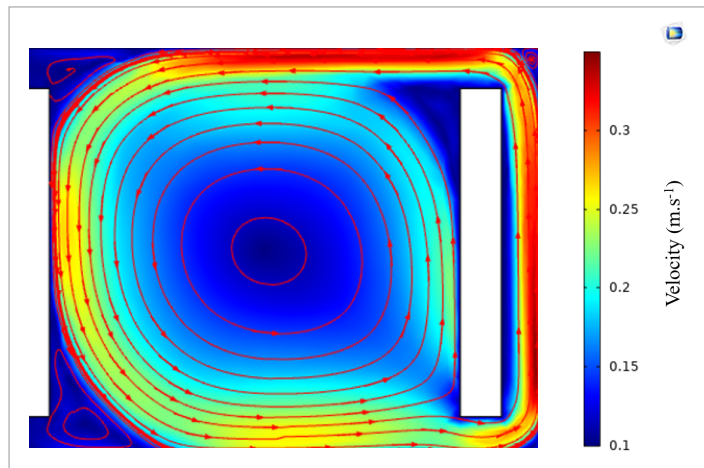


Fig. 8

Velocity field (Streamlines) and velocity magnitude (Surface) of a vertical cut plan at 04:00 PM in Ifrane city

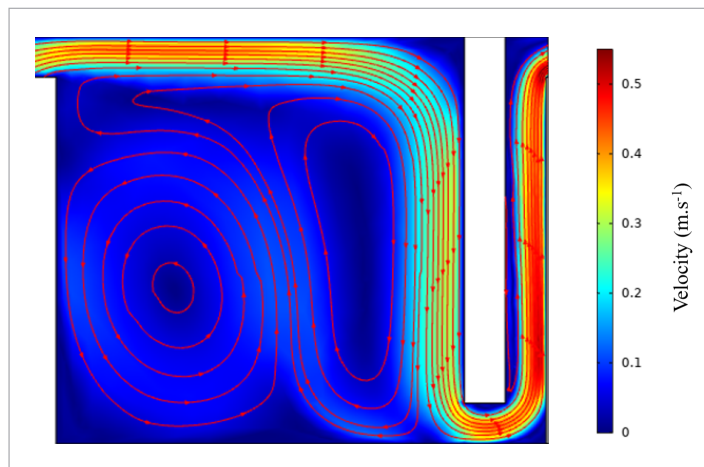


Fig. 9

Velocity field (Streamlines) and velocity magnitude (Surface) of a vertical cut plan at 04:00 PM in Marrakech city

During the winter, at the weather conditions of Ifrane (see Fig. 10), the volume flow rate varying between 201 m³/h and 224 m³/h, 246 m³/h and 270 m³/h, 238 m³/h and 261 m³/h, respectively, for Case 1, Case 4, and Case 2 configurations. By regarding the results in summer, Fig. 11 presents that generally, at Marrakech's weather conditions, a significant volume flow rate was recorded, which attained 303 m³/h, 348 m³/h, and 404 m³/h, respectively, for Case 1, Case 4, and Case 2 configurations.

By reading the details in Fig. 10 and 11, the three studied configurations showed, during the whole day, that the flow rate evolutions are taken the same with different amplitudes; this is explained by the different weather between the cities and the irregular Thermo-aeraulic behavior of each configuration.

An average volume flow rate estimation during 24 hours was carried out in the three configurations for the six cities corresponding to the climatic zones to choose the most adapted configurations around the year. Fig. 12 shows the three configurations' mean volume flow rate for the six Moroccan climate zones (Agadir, Tangier, Fez, Ifrane, Marrakech, and Er-rachidia) during summer and winter seasons.

In terms of natural ventilation, case 4 configuration is the most efficient during winter in all cities, followed by case 2 configuration and then the least efficient case 1 configuration. During the summer,

Fig. 10

Volume flow rate
in Ifrane city

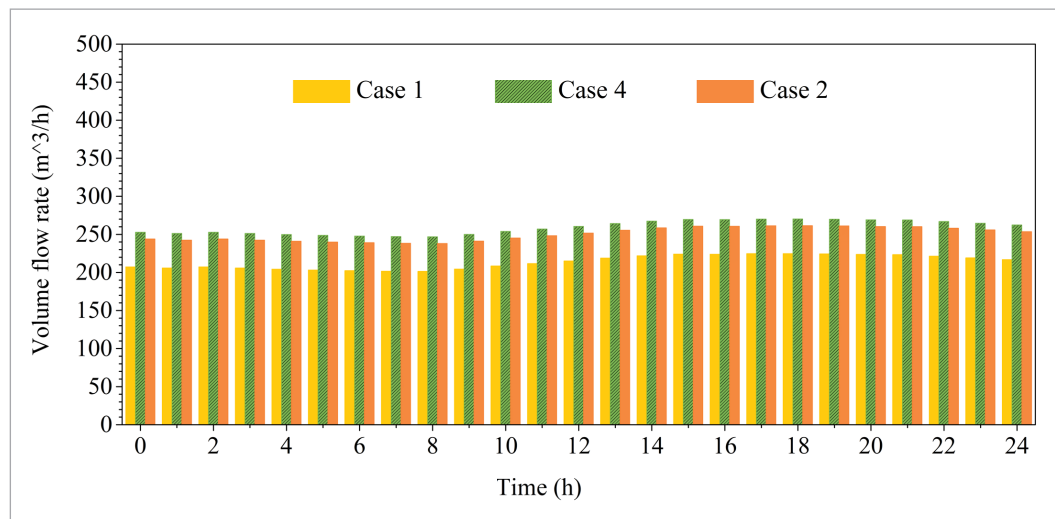
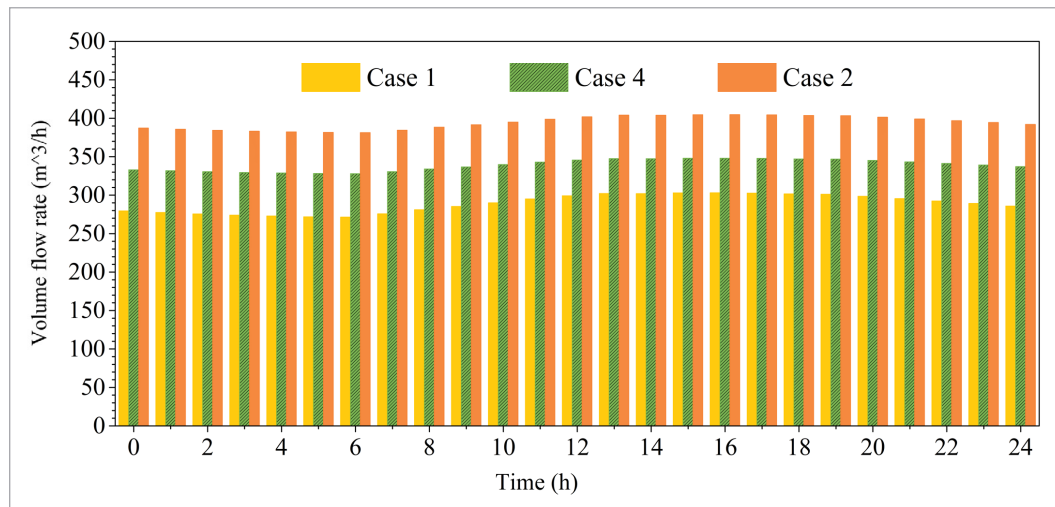


Fig. 11

Volume flow rate in
Marrakech city



we look at two groups of aerualic behavior; the first group (Agadir, Tangier, and Ifrane) in which case 4 configuration is the most efficient, followed by case 2 configuration, then the least efficient case 1 configuration. The second group (Fez, Marrakech, and Er-rachidia) in which case 3 configuration is the most efficient, followed by case 4 configuration, then the least efficient case 1 configuration.

In terms of comfort and energy efficiency, using Fig. 5, making from the literature review and the simulations carried out, we can conclude that case 1 configuration (Fig. 5-a), case 2 configuration (Fig. 5-b), and case 4 configuration (Fig. 5-d) is useful respectively for preheating, cooling, and heating.

Therefore, case 2 configuration is considered the only adaptive and most efficient for all climatic zones during the cooling season. For the heating season, the two case 1 and 4 configurations are well adapted, but the case 4 configuration is the most efficient.

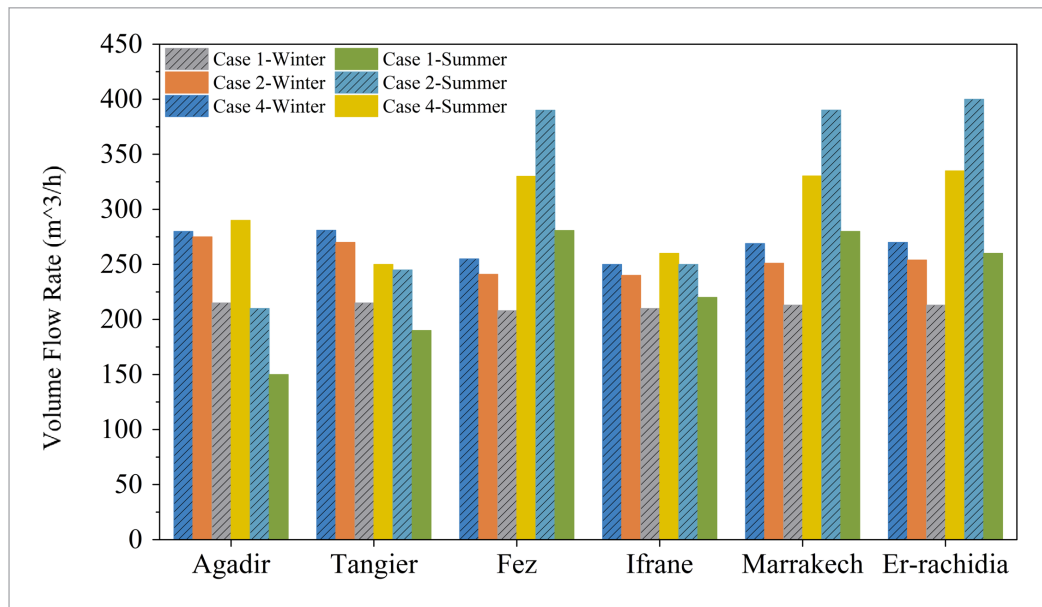


Fig. 12

Volume flow rate (m^3/h) for the six Moroccan climate zones

Through this study, we have performed a validated CFD simulation of different shapes from the Passive Second Skin Façade to assess its efficiency as a passive ventilation strategy in different Moroccan climate zones during cooling and heating seasons.

Simulation results revealed that the Case 4 configuration was considered the most suitable solution for the heating seasons; meanwhile, the Case 2 configuration has been verified most effectively during the cooling seasons. The recommended configurations can provide an average volume flow rate between $200 m^3/h$ and $400 m^3/h$ with a second-skin façade area of $1 m^2$ with an air vent area of $0.1m \times 0.2m$.

A better thermal comfort condition can be ensured by the Passive Second Skin Façade combined with other passive technologies, such as the geothermal exchanger, air radiative sky cooling system, and good sunshade during the summer months. Second Skin Façade may be considered a useful natural ventilation technique; regardless, more investigation of the parameters impacting its performance, like absorber surface, air gap thickness, air vent surface, and the glazing type, is required to integrate the building envelope.

These study results can also enhance the previous new design of Passive Façades and provide a reliable basis and useful reference for the future design and natural ventilation investigation of Passive Façades.

Conclusions and recommendations

References

- AB, C. (2020). COMSOL Multiphysics® (5.3a). www.comsol.com
- Abbassi, F., Dimassi, N., & Dehmani, L. (2014). Energetic study of a Trombe wall system under different Tunisian building configurations. *Energy and Buildings*, 80, 302-308. <https://doi.org/10.1016/j.enbuild.2014.05.036>
- AMEE. (2019). Agence Marocaine pour l'Efficacité Energétique. [Http://Www.Amee.Ma](http://Www.Amee.Ma).
- Bajc, T., Todorović, M. N., & Svorcan, J. (2015). CFD analyses for passive house with Trombe wall and impact to energy demand. *Energy and Buildings*, 98, 39-44. <https://doi.org/10.1016/j.enbuild.2014.11.018>
- Chel, A., Nayak, J. K., & Kaushik, G. (2008). Energy conservation in honey storage building using Trombe wall. *Energy and Buildings*, 40(9), 1643-1650. <https://doi.org/10.1016/j.enbuild.2008.02.019>
- Chen, B., Chen, X., Ding, Y. H., & Jia, X. (2006). Shading effects on the winter thermal performance of the Trombe wall air gap: An experimental study in Dalian. *Renewable Energy*, 31(12), 1961-1971. <https://doi.org/10.1016/j.renene.2005.07.014>
- Comsol. (2015). Heat Transfer Module. 1-222.
- Du, L., Ping, L., & Yongming, C. (2020a). Study and analysis of air flow characteristics in Trombe wall. *Renewable Energy*, 162, 234-241. <https://doi.org/10.1016/j.renene.2020.08.040>
- Du, L., Ping, L., & Yongming, C. (2020b). Study and analysis of air flow characteristics in Trombe wall. *Renewable Energy*, 162, 234-241. <https://doi.org/10.1016/j.renene.2020.08.040>
- Hong, X., Leung, M. K. H., & He, W. (2019). Thermal behaviour of Trombe wall with venetian blind in summer and transition seasons. *Energy Procedia*, 158(2018), 1059-1064. <https://doi.org/10.1016/j.egypro.2019.01.257>
- Hu, Z., Zhang, S., Hou, J., He, W., Liu, X., Yu, C., & Zhu, J. (2020). An experimental and numerical analysis of a novel water blind-Trombe wall system. *Energy Conversion and Management*, 205. <https://doi.org/10.1016/j.enconman.2019.112380>
- ISO 6946. (1996). Building components and building elements - Thermal resistance and thermal transmittance- Calculation method. 0. <https://doi.org/10.1111/j.1875-595X.2011.00062.x>
- Jaber, S., & Ajib, S. (2011). Optimum design of Trombe wall system in mediterranean region. *Solar Energy*, 85(9), 1891-1898. <https://doi.org/10.1016/j.solener.2011.04.025>
- Lin, Y., Ji, J., Zhou, F., Ma, Y., Luo, K., & Lu, X. (2019). *Energy & Buildings* Experimental and numerical study on the performance of a built-middle PV Trombe wall system. *Energy & Buildings*, 200, 47-57. <https://doi.org/10.1016/j.enbuild.2019.07.042>
- Liu, Y., Hou, L., Yang, Y., Feng, Y., Yang, L., & Gao, Q. (2020). Effects of external insulation component on thermal performance of a Trombe wall with phase change materials. *Solar Energy*, 204, 115-133. <https://doi.org/10.1016/j.solener.2020.04.010>
- Long, J., Jiang, M., Lu, J., & Du, A. (2019). Vertical temperature distribution characteristics and adjustment methods of a Trombe wall. *Building and Environment*, 165(August), 106386. <https://doi.org/10.1016/j.buildenv.2019.106386>
- Masson-Delmotte, V., Zhai, P., Pörtner, H. O., Roberts, D., Skea, J., Shukla, P. R., Pirani, A., Moufouma-Okia, W., Péan, C., Pidcock, R., Connors, S., Matthews, J. B., Chen, Y., Zhou, X., Gomis, M. I., Lonnoy, E., Maycock, T., Tignor, M., & Waterfield, T. (2018). Summary for Policymakers. In: *Global Warming of 1.5°C. An IPCC Special Report on the impacts of global warming of 1.5°C above pre-industrial levels and related global greenhouse gas emission pathways, in the context of strengthening the global response to.* In *Ipcc - Sr15*. https://report.ipcc.ch/sr15/pdf/sr15_spm_final.pdf <http://www.ipcc.ch/report/sr15/>
- Mehrzad Tabatabaian. (2014). COMSOL FOR Engineers.
- Nizovtsev, M. I., Letushko, V. N., Borodulin, V. Y., & Sterlyagov, A. N. (2020). Experimental studies of the thermo and humidity state of a new building facade insulation system based on panels with ventilated channels. *Energy and Buildings*, 206, 109607. <https://doi.org/10.1016/j.enbuild.2019.109607>
- Parhizkar, H., Khoraskani, R. A., & Tahbaz, M. (2020). Double skin façade with Azolla; ventilation, Indoor Air Quality and Thermal Performance Assessment. *Journal of Cleaner Production*, 249. <https://doi.org/10.1016/j.jclepro.2019.119313>
- Poirazis, H. (2004). *Double Skin Façades for Office Buildings Literature Review*.
- Prieto, A., Knaack, U., Auer, T., & Klein, T. (2018). Passive cooling & climate responsive façade design exploring the limits of passive cooling strategies to improve the performance of commercial buildings in warm climates. *Energy and Buildings*, 175, 30-47. <https://doi.org/10.1016/j.enbuild.2018.06.016>
- Stazi, F., Mastrucci, A., & di Perna, C. (2012). Trombe wall management in summer conditions: An experimental study. *Solar Energy*, 86(9), 2839-2851. <https://doi.org/10.1016/j.solener.2012.06.025>
- Trombe, F., & Michel, J. (1972). *NATURALLY AIR-CONDITIONED DWELLINGS*.

Vučenović, S. M., Fodor, K., Gut, I., & Šetrajčić, J. P. (2013). ACTIVE INSULATION - VARIATION OF TROMBE WALL. *Contemporary Materials*, 1(4), 62-68. <https://doi.org/10.7251/734>

Yu, T., Liu, B., Lei, B., Yuan, Y., Bi, H., & Zhang, Z. (2019). Thermal performance of a heating system combining solar air collector with hollow ventilated interior wall in residential buildings on Tibetan Plateau. *Energy*, 182, 93-109. <https://doi.org/10.1016/j.energy.2019.06.047>

Zalewski, L., Lassue, S., Duthoit, B., & Butez, M. (2002). Study of solar walls - Validating a simulation

model. *Building and Environment*, 37(1), 109-121. [https://doi.org/10.1016/S0360-1323\(00\)00072-X](https://doi.org/10.1016/S0360-1323(00)00072-X)

Zhou, Y., Wang, Z., Yang, C., Xu, L., Chen, W., Zhou, Y. A. N., Ā, Z. W., Yang, C., Xu, L., & Chen, W. E. I. (2019). Influence of Trombe wall on indoor thermal environment of a two-story building in rural Northern China during summer Influence of Trombe wall on indoor thermal environment of a two-story building in rural Northern China during summer. *Science and Technology for the Built Environment*, 0(0), 1-12. <https://doi.org/10.1080/23744731.2018.1550994>

YOUSSEF HAMIDI

Position at the organization

PhD. Student
Mohammed V University in Rabat,
École Nationale Supérieure
D'arts Et Métiers

Main research area

Energy efficiency, green building,
indoor environmental quality,
renewable energy

Address

ENSAM, B.P.6207, Rabat,
Morocco
Tel. +212 625 134 499
E-mail:
youssef.hamidi@um5s.net.ma

MUSTAPHA MALHA

Position at the organization

Full Professor
Mohammed V University in Rabat,
École Nationale Supérieure
D'arts Et Métiers

Main research area

Mechanical engineering,
materials sciences, renewable
energy

Address

ENSAM, B.P.6207, Rabat,
Morocco
Tel. +212 664 497 742
E-mail: m.malha@um5s.net.ma

ABDELLAH BAH

Position at the organization

Full Professor
Mohammed V University
in Rabat, École Nationale
Supérieure D'arts Et Métiers

Main research area

Energy efficiency, green building,
renewable energy

Address

ENSAM, B.P.6207, Rabat,
Morocco
Tel. +212 662 721 029
E-mail : a.bah@um5s.net.ma

About the Author



This article is an Open Access article distributed under the terms and conditions of the Creative Commons Attribution 4.0 (CC BY 4.0) License (<http://creativecommons.org/licenses/by/4.0/>).